5-Azacytidine and trichostatin A enhance the osteogenic differentiation of bone marrow mesenchymal stem cells isolated from steroid-induced avascular necrosis of the femoral head in rabbit

Peng Zhang[1], Fulin Tao[1], Qinghu Li[1], Shuai Wu[1], Baisheng Fu[1]* and Ping Liu[2]*

[1]*Department of Orthopaedics, Shandong Provincial Hospital Affiliated to Shandong University, 324 Jingwu Road, Jinan 250021, Shandong, People's Republic of China*

[2]*Department of Pharmacy, Shandong Provincial Hospital Affiliated to Shandong University, 324 Jingwu Road, Jinan 250021, Shandong, People's Republic of China*

*Corresponding author (Email, fubaisheng1986@163.com; liupingmedicine@163.com)

Bone marrow mesenchymal stem cells (BMSCs) play an important role in the process of bone repair. The present study investigated the effect of 5-azacytidine (AZA) and trichostatin A (TSA) on BMSC behaviors *in vitro*. The role of WNT family member 5A (WNT5A)/WNT family member 5A (WNT7A)/β-catenin signaling was also investigated. BMSCs were isolated from a steroid-induced avascular necrosis of the femoral head (SANFH) rabbit model. The third-generation of BMSCs was used after identification. The results revealed obvious degeneration and necrosis in the SANFH rabbit model. AZA, TSA and TSA + AZA increased BMSC proliferation in a time-dependent fashion. AZA, TSA and TSA + AZA induced the cell cycle release from the G0/G1 phase and inhibited apoptosis in BMSCs. AZA, TSA and TSA + AZA treatment significantly decreased caspase-3 and caspase-9 activities. The treatment obviously increased the activity and relative mRNA expression of alkaline phosphatase. The treatment also significantly up-regulated the proteins associated with osteogenic differentiation, including osteocalcin and runt-related transcription factor 2 (RUNX2), and Wnt/β-catenin signal transduction pathway-related proteins β-catenin, WNT5A and WNT7A. The relative levels of Dickkopf-related protein 1 (an inhibitor of the canonical Wnt pathway) decreased remarkably. Notably, TSA + AZA treatment exhibited a stronger adjustment ability than either single treatment. Collectively, the present studies suggest that AZA, TSA and TSA + AZA promote cell proliferation and osteogenic differentiation in BMSCs, and these effects are potentially achieved via up-regulation of WNT5A/WNT7A/β-catenin signaling.

Keywords. 5-Azacytidine; BMSCs; cell proliferation; trichostatin A; WNT/β-catenin signaling

1. Introduction

Avascular necrosis of the femoral head (ANFH) is a highly mutilating disease that is caused by multiple-etiologic factors (Meyers 1988; Smith 1997). Unfortunately, there are no effective treatments for femoral head ischemia.

Stem cells are immature cells that are not fully differentiated. These cells are known as 'universal cells' in the medical field and possess potential regenerative functions in multiple tissue types (Ulrich *et al.* 2013). Bone marrow mesenchymal stem cells (BMSCs) are key members of the stem cell family. These cells were originally identified in bone marrow and attracted increasing attention for several reasons, such as their multi-differentiation potential, hematopoietic support and promotion of immune regulation, self-replication and stem cell implantation (Hansson *et al.*

2004). BMSCs may differentiate into cells of various tissue types, such as fat, nerve, cartilage, muscle, bone, tendon, ligament, liver, endothelial tissues and cardiac muscle, under specific induction conditions *in vivo* and *in vitro*. BMSCs continue to exhibit multi-differentiation potential after successive subculture and cryopreservation. Therefore, these cells may be ideal seed cells for the repair of organ and tissue damage caused by disease or aging (Zeighami *et al.* 2014). BMSCs are promising stem cell candidates for translation into clinical treatment (Mahdavishahri *et al.* 2012).

5-Azacytidine (AZA) is a DNA-methylation inhibitor that is similar to cytidine. Previous research demonstrated its ability to alter cell fate and differentiate MSCs into cardiomyocytes via a peculiar molecular mechanism related to histone acetylation and DNA demethylation, which are key steps in the epigenetic modification of cells (Makino *et al.*

1999; Trojer and Reinberg 2006). Trichostatin A (TSA) was first reported as a potent histone deacetylase (HDAC) inhibitor, and it chelates the central zinc-finger motif of HDACs to inhibit enzyme activity (Tsuji *et al.* 1976; Yoshida *et al.* 1990). TSA improved the survival in a rat model of hemorrhagic shock (Lin *et al.* 2007). AZA + TSA treatment rescued the cell viability of lipopolysaccharides (LPS)-induced bone marrow-derived macrophages (Thangavel *et al.* 2015). TSA is generally used as a reagent in epigenetics research. Numerous studies demonstrated the biological activities of TSA (Thangavel *et al.* 2015; Miyake *et al.* 2016). However, fewer studies reported the effects of AZA and TSA treatment individually and in combination on BMSC behaviors *in vitro* and *in vivo*. The potential molecular mechanism is not defined.

The canonical Wnt pathway (or Wnt/β-catenin pathway) is the Wnt pathway that leads to an accumulation of intracellular β-catenin and its eventual translocation into the nucleus to act as a transcriptional co-activator of transcription factors (Pardal *et al.* 2003). Wnt signaling plays a critical role in embryonic development, axis patterning, cell fate specification, cell proliferation and cell migration (Kaldis and Pagano 2009; Micalizzi *et al.* 2010; Vasiev *et al.* 2010). However, few studies reported the effects of the canonical Wnt pathway on the osteogenic differentiation of BMSCs, and the potential molecular mechanism is not defined.

Therefore, the present research investigated the effects of AZA and TSA treatment alone and in combination on BMSC behaviors *in vitro*. Proteins related to the WNT/β-catenin signaling pathway (Wnt family member 5A, WNT5A, Wnt family member 7A, WNT7A and β-catenin) were also investigated.

2.   Materials and methods

2.1   *Chemicals and reagents*

Hematoxylin–eosin (H&E) staining kits were purchased from Beyotime Biotech (Shanghai, China). Primary antibodies for osteocalcin (OCN), cleaved caspase 3, cleaved caspase 9, ALP and glyceraldehyde-3-phosphate dehydrogenase (GAPDH) were purchased from Abcam Biotech (Cambridge, MA, USA). Primary antibodies for Dickkopf-related protein 1 (DKK-1), β-catenin, RUNX2 and WNT5A were purchased from Aviva Systems Biology (San Diego, CA, USA). The primary WNT7A antibody was purchased from Bioss (Beijing, China). Trizol reagents were purchased from Invitrogen (Carlsbad, CA, USA). AZA and TSA were acquired from Sigma-Aldrich (St. Louis, MO, USA), and 98% purity was detected by high-performance liquid chromatography analysis. Biochemical assay kits for alkaline phosphatase (ALP), caspase-3 and caspase-9 were purchased from KeyGEN Bio (Nanjing, China).

2.2   *Animals*

New Zealand white rabbits (3.5 ± 0.5 kg) were obtained from the Shanghai Laboratory Animal Center (Shanghai, China). The experiments were performed in accordance with the Animal Ethics Committee of our hospital. All rabbits were maintained in temperature-controlled housing ($25 \pm 1°C$) with free access to food and water. The animal model was established according to a previous report (Noa *et al.* 2012). Twelve rabbits were randomly allocated to two groups ($n = 6$ per group): sham group and steroid-induced ANFH (SANFH) group. SANFH group rabbits were injected with 10 µg/kg LPS (Sigma-Aldrich, St. Louis, MO, USA) daily via ear vein injection for 1 day. Prednisolone acetate (20 mg/kg, Sigma-Aldrich, St. Louis, MO, USA) was injected into the right gluteus medius muscle daily for 3 days. Rabbits in the sham group received equal amounts of normal saline. Rabbits in the sham and SANFH groups were sacrificed by ketamine (40 mg/kg) and xylazine (3.5 mg/kg) at 2, 4 and 6 weeks after surgery (2 rabbits per time point in each group), and femoral head tissues were collected.

2.3   *BMSCs*

BMSCs were isolated from bone marrow at 6 weeks after surgery and cultured as previously described (Wang *et al.* 2017). Autologous primary MSCs were collected from 15 to 20 µL of bone marrow extracted from each experimental animal using 5 mL of α-minimum essential medium (Invitrogen Life Technologies, Carlsbad, CA, USA) with a 25-gauge needle followed by gradient centrifugation. After microscopic examination, the second-generation MSCs were plated into a six-well plate and incubated with low-glucose complete Dulbecco's modified Eagle's medium (Invitrogen Life Technologies) containing 10% fetal bovine serum and 100 U/mL penicillin/streptomycin (Invitrogen Life Technologies) in a humidified atmosphere at 37°C with 5% CO_2. Cells were split when they reached 80% confluence, and the third passage was used in subsequent experiments.

Third-generation BMSCs were incubated for 1 h at 4°C with CD29, CD44 and CD45 (Becton-Dickinson, San Diego, CA, USA) antibodies. BMSCs in the negative control group were incubated with IgG1 antibodies (BD Pharmingen, US). Primary antibodies labeled with fluorescein isothiocyanate (FITC) were added and incubated for 1 h at 4°C. The labeled cells were analyzed using flow cytometry.

BMSCs were isolated from SANFH rabbits and divided into four groups: model, AZA, TSA and TSA + AZA. BMSCs isolated from sham rabbits served as the normal control (NC) group. BMSCs in the AZA, TSA and TSA + AZA groups (dissolved in dimethyl sulfoxide, DMSO) were treated with AZA (1.25 µM), TSA (0.1 µM) and TSA + AZA (1.25 µM AZA and 0.1 µM TSA), respectively, for 72 h. BMSCs in the NC and model groups were treated with equal amounts of solvent.

2.4 *Histopathological examinations*

Histopathological examinations were performed according to a previous report with minor modification (Peng *et al.* 2015). Briefly, femoral head tissues were fixed in 10% neutral-buffered formalin. Standard methods of dehydration, clearing in xylene and paraffin embedding were used. Sections (5 μm thickness) were cut using a rotary microtome. Sections were de-paraffinized, and femoral head tissue sections were stained using a H&E staining kit. Histopathological changes were observed under an optical microscope (Olympus, Japan).

2.5 *Cell proliferation, apoptosis and cell cycle of BMSCs in different groups*

The effects of AZA, TSA and TSA + AZA on the proliferation of BMSCs were examined using a CCK-8 assays kit (SAB, Maryland, USA) 0, 24, 48 and 72 h after treatment.

The effects of AZA, TSA and TSA + AZA on cell apoptosis were determined using FITC-labeled annexin-V/propidium iodide (PI) double staining (Sigma). Cells (1×10^6) were treated for 72 h and incubated with FITC-labeled annexin-V and PI for 15 min at room temperature. The intensity of annexin-V or PI fluorescence was analyzed using FACScan (Becton-Dickinson, San Diego, CA, USA), and 10,000 cells were evaluated in each sample.

The cells (1×10^5) were seeded and further starved in serum-free medium to synchronize cell cycle progression. The starved cells were treated with DMSO, AZA, TSA and TSA + AZA for 72 h, harvested and fixed in 70% methanol at 4°C overnight. The fixed cells were incubated with RNase (10 mg/mL) and PI (1 mg/mL) (Sigma) at room temperature in the dark for 30 min. The DNA content was analyzed using

FACScan (Becton-Dickinson, San Diego, CA, USA) and FLOWJO software (Stanford University's Leonard Herzenberg Lab, Stanford, CA, USA).

2.6 *ALP, caspase-3 and caspase-9 activities in BMSCs*

The relative activities of ALP, caspase-3 and caspase-9 in BMSCs were examined using the colorimetric method.

Total protein was extracted from BMSCs 72 h after incubation. The relative activities of ALP in BMSCs were measured using colorimetric assay kits according to the manufacturer's instructions.

The cells were washed twice in phosphate-buffered saline after treatment, and $3–5 \times 10^6$ cells were collected. The cells were dissolved in precooled lysis buffer (100 μL), and the supernatant was collected for caspase-3 and caspase-9 assays. The supernatant (50 μL) was mixed with 50 μL of reaction buffer (2×), and the caspase-3/caspase-9 substrate (5 μL) was added. The cells were incubated in the dark at 37°C for 4 h. Absorbance was measured at 400 nm using a microplate reader. Relative caspase-3/caspase-9 was obtained via calculation of the ratio to the reference standard. The results were expressed as the ratio of optical density of groups to the reference standard.

2.7 *Quantitative real-time polymerase chain reaction (PCR)*

ALP expression was determined using real-time PCR after 72 h of incubation. Total RNA (2 μg of each sample) was extracted from BMSCs and reverse transcribed to cDNA using reverse transcription kits (Thermo, MA, USA). The obtained cDNA was used as a template for real-time PCR
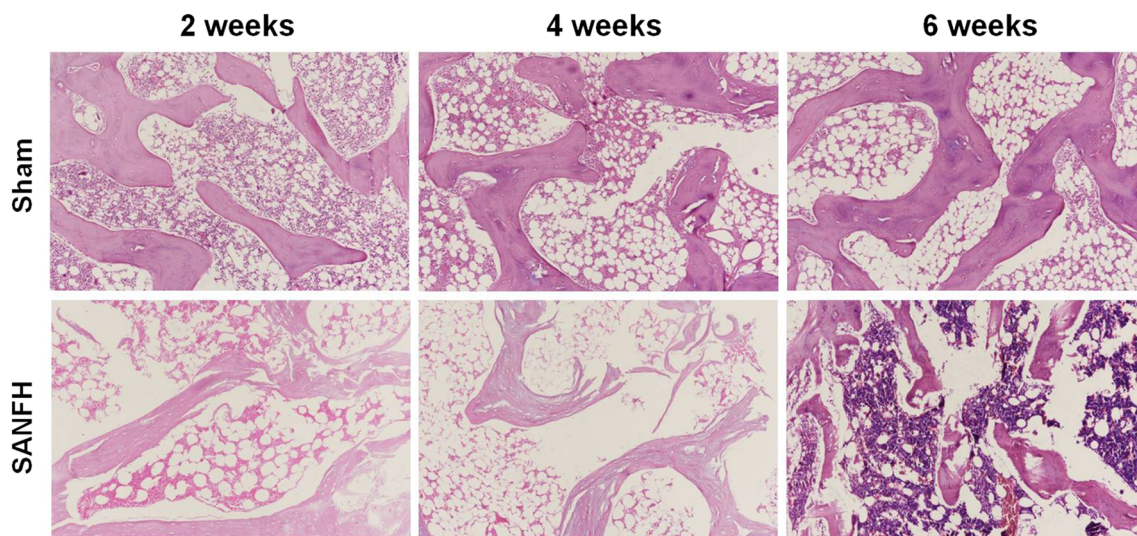

Figure 1. Results of H&E staining in the NC group and SANFH model group at 2, 4 and 6 weeks after treatment (*n* = 3). Magnification: 100×.
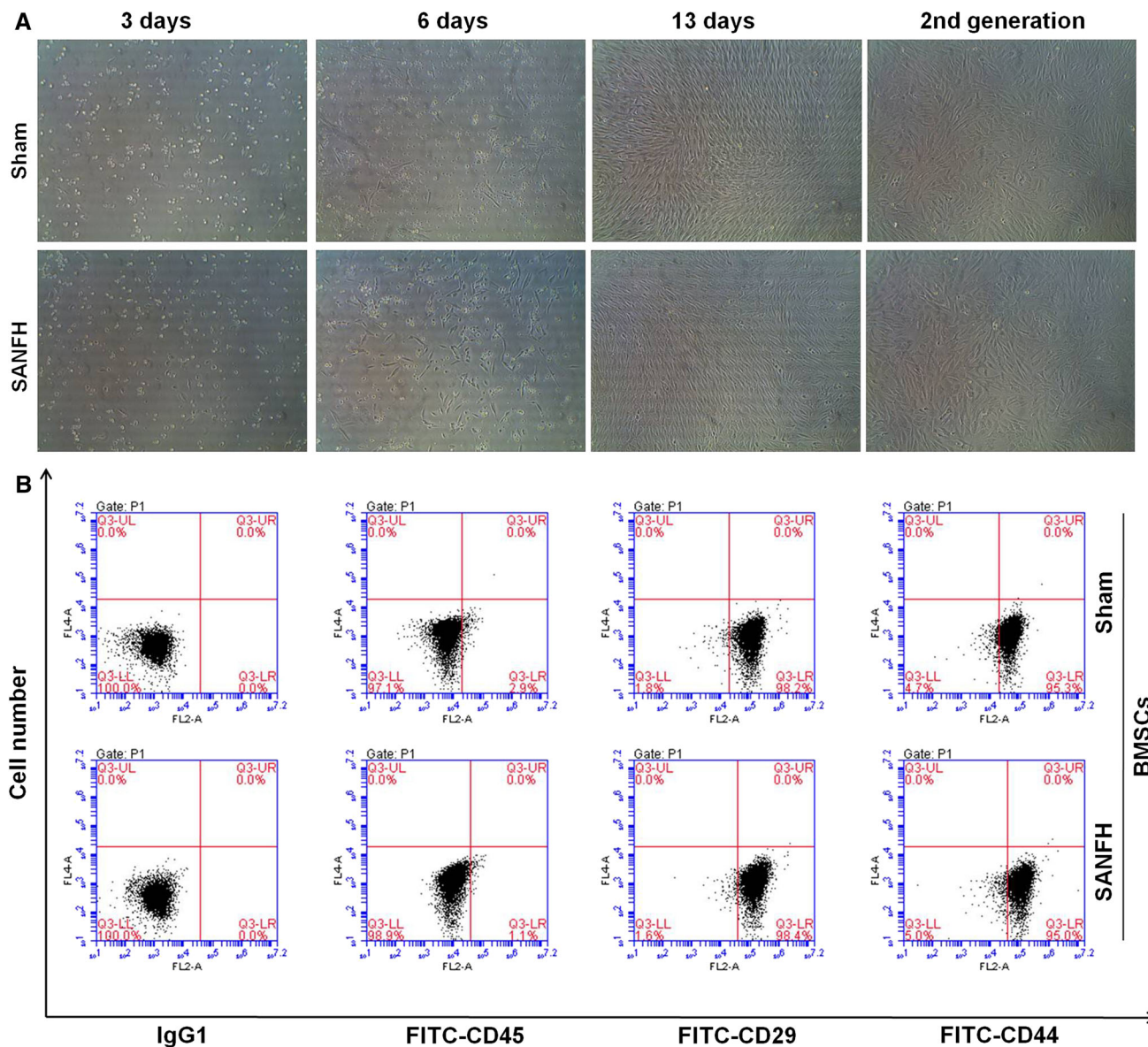
Figure 2. (**A**) Microscopic examination of the isolated BMSCs (3, 6 and 13 days after incubation and the second-generation cells). Magnification: 200×. (**B**) The identification of the third-generation BMSCs using flow cytometry. BMSCs were positive for cell surface markers CD44 and CD29 and negative for CD45 ($n = 3$).

analysis in a quantitative real-time PCR machine (ABI-7300, USA) using SYBR Green reagents (Thermo, MA, USA).

Primers for the real-time PCR were designed in Primer 5.0 and synthesized by JRDun Biotech (Shanghai, China). The primer sequences are: ALP (forward: 5′ ACAAGCACTCC CACTTTGTC 3′; reverse: 5′ TTCAGCTCGTACTGCAT GTC 3′) and GAPDH (forward: 5′ GTCGGAGTGAACGG ATTTG 3′; reverse: 5′ ATCTCGCTCCTGGAAGATG 3′). Relative mRNA expression was evaluated by $2^{-\Delta\Delta Ct}$ relative quantitative analysis for each sample against GAPDH gene expression: $\Delta\Delta Ct$ = (Ct, target gene in the treated group – Ct, reference gene in the treated group) – (Ct, target gene in the control group – Ct, reference gene in the control group).

2.8   *Western blotting assay*

Protein expression levels of extracellular secreted DKK-1, intracellular OCN, β-catenin, runt-related transcription factor 2 (RUNX2), cleaved caspase 3, cleaved caspase 9, ALP, WNT5A and WNT7A were determined by Western blotting.

Total protein was extracted from BMSCs (from collected conditioned media for the detection of DKK-1) 72 h after incubation, separated by SDS-PAGE and transferred onto PVDF membranes, as previously described (Blumer *et al.* 2008). The membranes were incubated with a primary antibody overnight at 4°C, followed by a secondary antibody for 2 h at 4°C. Protein bands were detected by using an ECL-

detecting kit (Beyotime Biotech, Shanghai, China). Each blot was normalized to its corresponding internal control (GAPDH) value.

2.9 *Statistical analysis*

All data are expressed as the means $\pm$ SD. ANOVA and Duncan's multiple range test were performed to compare the differences between two groups using SPSS 20.0 software (SPSS Inc., USA). *P* values less than 0.05 were recognized as significant.

3. Results

3.1 *Histopathological examination*

Histopathological abnormalities in femoral head tissues were examined at the end of animal experiments using H&E staining. Intramedullary cells and trabecular bone normally existed for 2, 4 and 6 weeks post-surgery in NC rabbits, and there were no empty lacunae cells (figure 1). However, trabecular bone fractures and empty lacunae cells appeared in the SANFH group, and the architecture of marrow tissue had deteriorated. A large amount of BMC necrosis was observed, and normal bone marrow architecture nearly disappeared at 6 weeks.

3.2 *Identification of BMSCs*

The morphological images of isolated BMSCs after 3, 6 and 13 days of incubation and the second generation of isolated BMSCs were obtained using an optical microscope (figure 2A).

 Flow cytometry indicated that CD29- and CD44-positive cells comprised 98.4 and 95.0%, respectively, of cells in the SANFH group, 98.3 and 95.2% of cells in the control group. CD45 staining was negative in the third-generation BMSCs (figure 2B). These results suggested that most cells were BMSCs after three generations in subculture.

3.3 *AZA, TSA and TSA + AZA promote cell proliferation of BMSCs*

The effects of AZA, TSA and TSA + AZA on BMSC proliferation were investigated using CCK-8 assays. The results indicated that AZA, TSA and TSA + AZA increased BMSC proliferation at 48 and 72 h after incubation (figure 3). However, no significant differences were observed in the AZA treatment groups compared to the model group at 24 h. The combined treatment more significantly affected BMSC proliferation than single treatment.
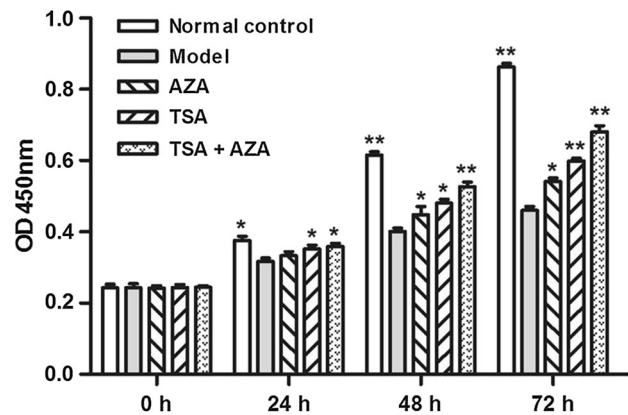

Figure 3. Effects of AZA, TSA and TSA + AZA on BMSC proliferation (CCK-8 assay). Data are shown as the means $\pm$ sd. *$p<0.05$, **$p<0.01$, compared to the model group at the same time ($n = 3$).

3.4 *AZA, TSA and TSA + AZA induced the release of cell cycle from the G0/G1 phase and inhibited apoptosis in BMSCs*

AZA, TSA and TSA + AZA treatment significantly increased the BMSC proliferation. Therefore, the effects of AZA, TSA and TSA + AZA on cell cycle regulation and cell death were investigated. The cell cycle of BMSCs was arrested in the G0/G1 phase in the model group, and AZA, TSA and TSA + AZA treatment remarkably improved this arrest (figure 4). AZA, TSA and TSA + AZA treatment significantly reduced apoptosis in BMSCs compared to the model group (figure 5A).

 Caspase-9 and caspase-3 play distinct roles in intrinsic apoptotic pathways (Brentnall *et al.* 2013). The relative activities as well as protein levels of caspase-3 and caspase-9 were measured 72 h after AZA, TSA and TSA + AZA treatment in BMSCs. AZA, TSA and TSA + AZA treatment remarkably decreased caspase-3 and caspase-9 activities (figure 5B and C). The combined treatment was more effective than the single treatments (figure 5).

3.5 *AZA, TSA and TSA + AZA up-regulated the expression and activity of ALP in BMSCs*

ALP is a necessary enzyme in the osteogenesis process. ALP expression indicates the state of osteogenesis and correlates with osteoblast differentiation and maturation (Bose *et al.* 2010). Relative protein levels, mRNA expression and ALP activity in BMSCs were determined after AZA, TSA and TSA + AZA treatment. AZA, TSA and TSA + AZA treatment remarkably increased the protein level, relative mRNA expression and ALP activity. The combined treatment was significantly effective than the single treatment (figures 5C and 6).
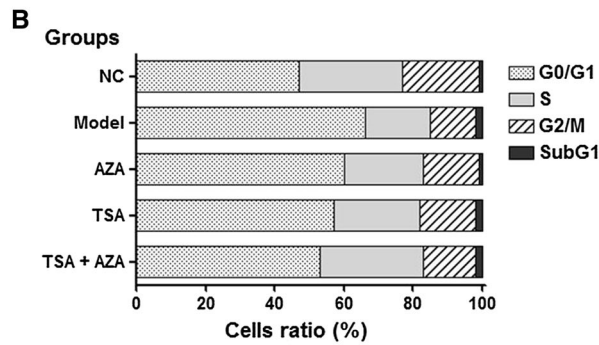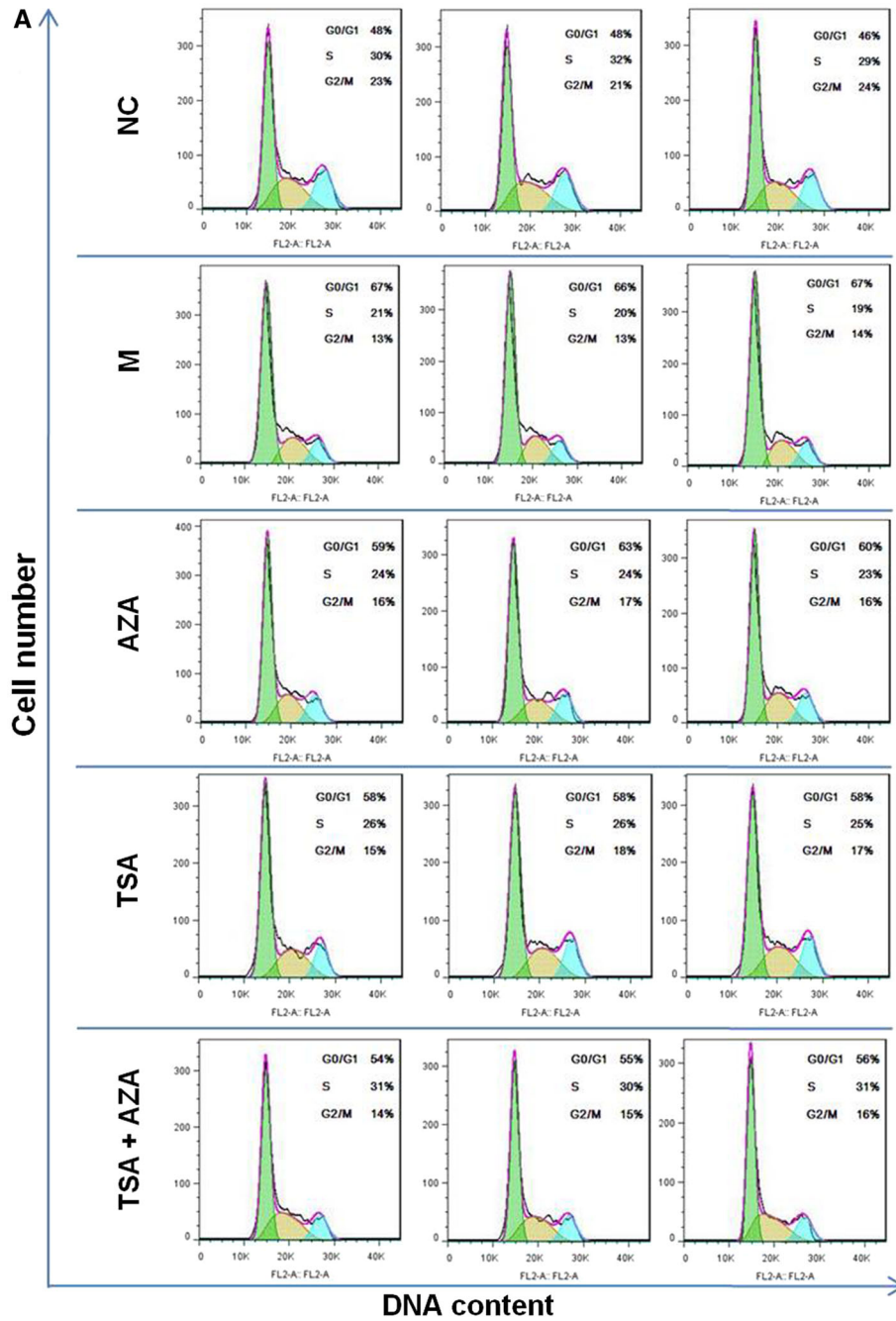
Peng Zhang et al.

Figure 4. AZA, TSA and TSA + AZA regulates the cell cycle in BMSCs. BMSCs were incubated for 72 h after treatment, and the cell cycle was analyzed using flow cytometry ($n = 3$).
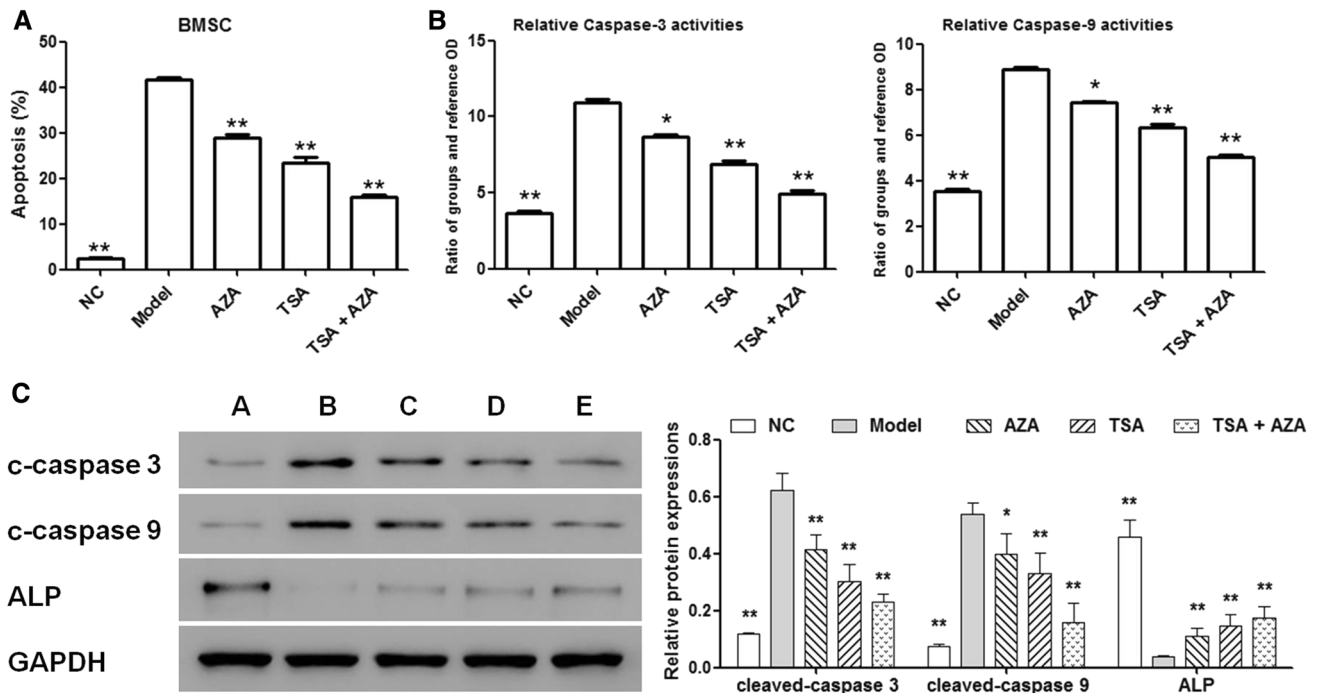
Figure 5. Apoptosis reduction was observed in BMSCs under AZA, TSA and TSA + AZA treatment for 72 h (**A**). Relative activities of caspase-3 and caspase-9 were reduced in BMSCs under treatment. The results were expressed as the ratio of optical density of groups to the reference standard (**B**). Protein levels of cleaved caspase 3, cleaved caspase 9 and ALP in BMSCs under treatment (**C**) (A: NC, B: model, C: AZA, D: TSA, E: TSA + AZA). Data are shown as the means $\pm$ sd. *p<0.05, **p<0.01, compared to the model group (n = 3).
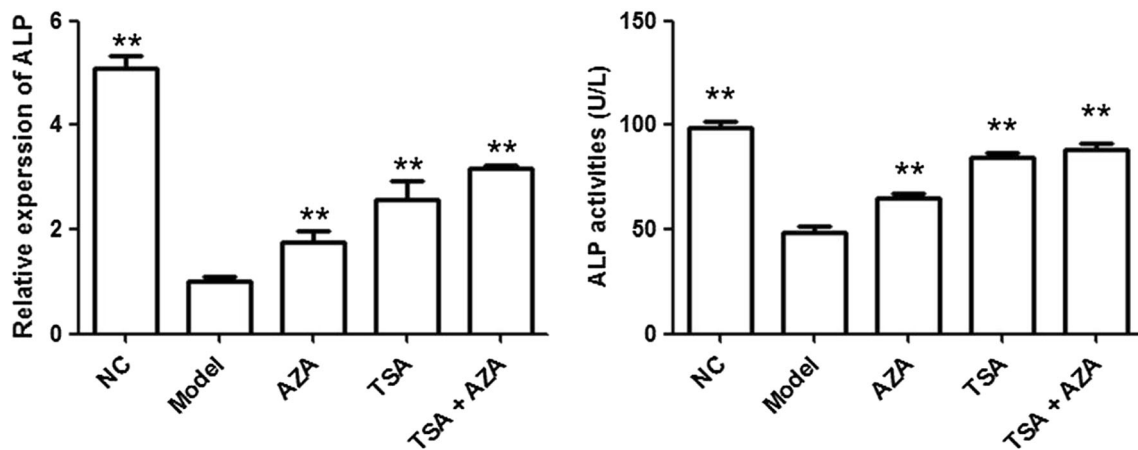

Figure 6. Relative mRNA expression and activity of ALP in BMSCs under AZA, TSA and TSA + AZA treatment. Data are shown as the means $\pm$ sd. *p<0.05, **p<0.01, compared to the model group (n = 3).

3.6 *Protein expression of DKK-1, OCN, β-catenin, RUNX2, WNT5A and WNT7A*

Proteins associated with osteogenic differentiation, OCN (Qiu *et al.* 2014) and RUNX2 (Fensky *et al.* 2014) and Wnt/β-catenin signal transduction pathway-related proteins DKK-1 (Glinka *et al.* 1998), β-catenin, WNT5A and WNT7A were determined using Western blotting.

AZA, TSA and TSA + AZA treatment remarkably up-regulated the relative protein levels of OCN, β-catenin, RUNX2, WNT5A and WNT7A in BMSCs (figure 7). In

contrast, the relative protein levels of DKK-1 decreased remarkably. The TSA + AZA treatment group exhibited stronger adjustment ability than single treatment.

4. Discussion

The steroid-induced ANFH rabbit model used in the present study successfully induced osteonecrosis as indicated by histological examinations, and this finding is consistent with a previous report (Yuan *et al.* 2015). The present study
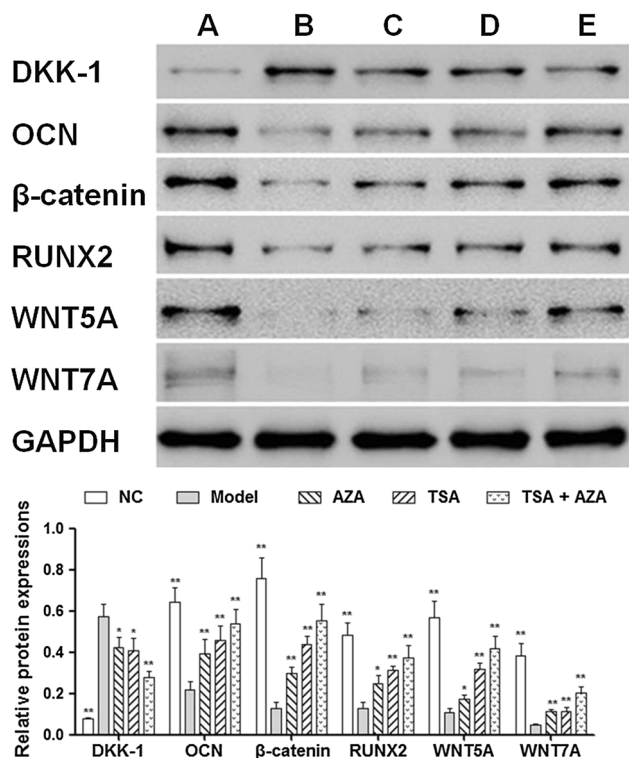
Figure 7. Effects of different treatments on protein expression of DKK-1, OCN, β-catenin, RUNX2, WNT5A and WNT7A in BMSCs (A: NC, B: model, C: AZA, D: TSA, E: TSA + AZA). Data are shown as the means ± sd. *$p<0.05$, **$p<0.01$, compared to the model group ($n = 3$).

suggests that AZA, TSA and TSA + AZA promote cell proliferation, induce the release of the cell cycle from the G0/G1 phase and inhibit apoptosis in BMSCs. AZA, TSA and TSA + AZA treatment enhanced osteogenic differentiation in BMSCs via up-regulation of WNT5A/WNT7A/β-catenin signaling. The possible mechanism involves the up-regulation of WNT5A/WNT7A/β-catenin signaling.

BMSCs secrete DKK-1 in the lag phase, and it is an active component of the conditioned medium that stimulates the progression of cells into the log phase (Horwitz 2004). DKK-1 is also an inhibitor of the canonical Wnt pathway (Glinka et al. 1998). The present results indicated that the relative protein expression of DKK-1 was extremely higher in the model group, and AZA, TSA and TSA + AZA treatment significantly down-regulated DKK-1. The cell cycle of BMSCs was arrested at the G0/G1 phase in the model group. However, treatment remarkably improved this symptom. AZA, TSA and TSA + AZA induced the release of cell cycle from the G0/G1 phase.

Caspase-3 is an index of apoptosis, and it is a critical mediator of the execution phase of cell apoptosis. Caspase-3 is involved in many different pathways, including the cleaving of DNA repair molecules, skeleton proteins, and extracellular matrix proteins, and the degradation of anti-apoptotic proteins (Zheng et al. 1998). Caspase-9 and

caspase-3 play distinct roles in intrinsic apoptotic pathways. Mitochondria-released cytochrome c activates caspase-9, which activates caspase-3 (Brentnall et al. 2013). Caspase-9 directly interacts with p5 in vitro, and lower cellular expression of p53 correlates with lowered caspase-9 activity (Chee et al. 2013). Our results demonstrated that AZA, TSA and TSA + AZA treatment significantly reduced apoptosis in BMSCs compared to the model group, and treatment remarkably reduced the relative activation of caspase-9 and caspase-3. It may be related to the reduced expression of p53, and this hypothesis will be verified in future experiments.

OCN is a K-dependent calcium-binding protein that is synthesized and secreted by osteoblasts, and it plays an important role in the process of bone repair (Qiu et al. 2014). RUNX2 was studied most extensively as a crucial factor in the osteogenic process. RUNX2 expression promotes the osteogenic differentiation of MSCs (Fensky et al. 2014). ALP is a necessary enzyme in the osteogenesis process. ALP hydrolyzes organic phosphate to release inorganic phosphate, which forms hydroxyapatite. ALP expression indicates a state of osteogenesis, i.e., the beginning of osteoblast differentiation, and it positively correlates with osteoblast differentiation and maturation (Bose et al. 2010). The present results indicated that the protein expression of OCN and RUNX2, and treatment obviously up-regulated the mRNA expression and activity of ALP. These results demonstrated that AZA, TSA and TSA + AZA promoted osteogenic differentiation in BMSCs.

Wnt signaling is indispensable for orchestrating the complex cell behaviors that occur throughout development (Croce and McClay 2008). Wnt signaling controls cell proliferation, stem cell maintenance and cell fate decisions, and it organizes cell movements and the establishment of tissue polarity (van Amerongen and Nusse 2009). Wnt6, Wnt10a and Wnt10b inhibit adipogenesis and stimulate osteoblastogenesis via a β-catenin-dependent mechanism (Cawthorn et al. 2012). The inhibition of DNA methylation switches adipogenesis to osteoblastogenesis via the activation of Wnt10a in mesenchymal stem cells, and treatment of 5-Aza-dC increases the β-catenin content at the early stage of differentiation (Chen et al. 2016). The present results indicated that AZA, TSA and TSA + AZA treatment significantly up-regulated the protein expression of β-catenin, WNT5A and WNT7A in BMSCs. These results indicate that WNT5A/WNT7A/β-catenin signaling is a potential mechanism related to the process of SANFH and osteogenic differentiation.

In conclusion, the present study revealed that AZA, TSA and TSA + AZA treatment promoted the cell proliferation of BMSCs isolated from SAFNH rabbits. The possible mechanism involves the up-regulation of WNT5A/WNT7A/β-catenin signaling. Treatments induced the release of the cell cycle from the G0/G1 phase and inhibited apoptosis. AZA, TSA and TSA + AZA treatment up-regulated the mRNA (ALP), proteins (OCN and RUNX2) and enzyme activity

(ALP) related to the process of bone repair. The possible mechanism involves the up-regulation of WNT5A/WNT7A/β-catenin signaling. The TSA + AZA treatment group exhibited stronger adjustment ability. AZA and TSA treatment individually or in combination may be a potential treatment for ANFH.

Acknowledgements

References

Blumer MJ, Longato S and Fritsch H 2008 Structure, formation and role of cartilage canals in the developing bone. *Ann. Anat.* **190** 305–315

Bose R, Moors M, Tofighi R, Cascante A, Hermanson O and Ceccatelli S 2010 Glucocorticoids induce long-lasting effects in neural stem cells resulting in senescence-related alterations. *Cell Death Dis.* **1** e92

Brentnall M, Rodriguez-Menocal L, De Guevara RL, Cepero E and Boise LH 2013 Caspase-9, caspase-3 and caspase-7 have distinct roles during intrinsic apoptosis. *BMC Cell Biol.* **14** 32

Cawthorn WP, Bree AJ, Yao Y, Du B, Hemati N, Martinez-Santibañez G and MacDougald OA 2012 Wnt6, wnt10a and wnt10b inhibit adipogenesis and stimulate osteoblastogenesis through a β-catenin-dependent mechanism. *Bone* **50** 477–489

Chee JLY, Saidin S, Lane DP, Leong SM, Noll JE, Neilsen PM, Yi TP, Gabra H and Lim TM 2013 Wild-type and mutant p53 mediate cisplatin resistance through interaction and inhibition of active caspase-9. *Cell Cycle* **12** 278–288

Chen YS, Wu R, Yang X, Kou S, Macdougald OA, Yu L, Shi H and Xue B 2016 Inhibiting DNA methylation switches adipogenesis to osteoblastogenesis by activating wnt10a. *Sci. Rep.* **6** 25283

Croce JC and McClay DR 2008 Evolution of the wnt pathways. *Methods Mol. Biol.* **469** 3–18

Fensky F, Reichert JC, Traube A, Rackwitz L, Siebenlist S and Noth U 2014 Chondrogenic predifferentiation of human mesenchymal stem cells in collagen type i hydrogels. *Biomedizinische Technik/Biomed. Eng.* **59** 375–383

Glinka A, Wu W, Delius H, Monaghan AP, Blumenstock C and Niehrs C 1998 Dickkopf-1 is a member of a new family of secreted proteins and functions in head induction. *Nature* **391** 357–362

Hansson M, Tonning A, Frandsen U, Petri A, Rajagopal J, Englund MC, Heller RS, Hakansson J, Fleckner J, Skold HN, Melton D, Semb H and Serup P 2004 Artifactual insulin release from differentiated embryonic stem cells. *Diabetes* **53** 2603–2609

Horwitz EM 2004 Dkk-1-mediated expansion of adult stem cells. *Trends Biotechnol.* **22** 386–388

Kaldis P and Pagano M 2009 Wnt signaling in mitosis. *Dev. Cell* **17** 749–750

Lin T, Chen H, Koustova E, Sailhamer EA, Li Y, Shults C, Liu B, Rhee P, Kirkpatrick J and Alam HB 2007 Histone deacetylase as therapeutic target in a rodent model of hemorrhagic shock: Effect of different resuscitation strategies on lung and liver. *Surgery* **141** 784–794

Mahdavishahri N, Moghatam Matin M, Fereidoni M, Yarjanli Z, Banihashem Rad SA and Khajeh Ahmadi S 2012 *In vitro* assay of human gingival scaffold in differentiation of rat's bone marrow mesenchymal stem cells to keratinocystes. *Iran. J. Basic. Med. Sci.* **15** 1185–1190

Makino S, Fukuda K, Miyoshi S, Konishi F, Kodama H, Pan J, Sano M, Takahashi T, Hori S, Abe H, Hata J, Umezawa A and Ogawa S 1999 Cardiomyocytes can be generated from marrow stromal cells *in vitro*. *J. Clin. Invest.* **103** 697–705

Meyers MH 1988 Osteonecrosis of the femoral head. Pathogenesis and long-term results of treatment. *Clin. Orthop. Relat. Res.* **231** 51–61

Micalizzi DS, Farabaugh SM and Ford HL 2010 Epithelial-mesenchymal transition in cancer: Parallels between normal development and tumor progression. *J. Mammary. Gland. Biol. Neoplasia.* **15** 117–134

Miyake Y, Keusch JJ, Wang L, Saito M, Hess D, Wang X, Melancon BJ, Helquist P, Gut H and Matthias P 2016 Structural insights into hdac6 tubulin deacetylation and its selective inhibition. *Nat. Chem. Biol.* **12** 748–754

Noa M, Más R, Valle M, Mendoza S and Mendoza N 2012 Effect of d-003, a mixture of high molecular weight aliphatic acids, on glucocorticoid- and lipopolysaccharides (lps)-induced osteonecrosis. *Iran. J. Pharm. Res.: IJPR* **11** 1201–1208 *http://www.ncbi.nlm. nih.gov/pmc/articles/PMC3813174/*

Pardal R, Clarke MF and Morrison SJ 2003 Applying the principles of stem-cell biology to cancer. Nature reviews. *Cancer* **3** 895–902

Peng W, Qiu X-Q, Shu Z-H, Liu Q-C, Hu M-B, Han T, Rahman K, Qin L-P and Zheng C-J 2015 Hepatoprotective activity of total iridoid glycosides isolated from paederia scandens (lour.) merr. Var. Tomentosa. *J. Ethnopharmacol.* **174** 317–321 *http://www. sciencedirect.com/science/article/pii/S0378874115301045*

Qiu X, Jin X, Shao Z and Zhao X 2014 17beta-estradiol induces the proliferation of hematopoietic stem cells by promoting the osteogenic differentiation of mesenchymal stem cells. *Tohoku. J. Exp. Med.* **233** 141–148

Smith DW 1997 Is avascular necrosis of the femoral head the result of inhibition of angiogenesis? *Med. Hypotheses* **49** 497–500

Thangavel J, Samanta S, Rajasingh S, Barani B, Xuan YT, Dawn B and Rajasingh J 2015 Epigenetic modifiers reduce inflammation and modulate macrophage phenotype during endotoxemia-induced acute lung injury. *J. Cell Sci.* **128** 3094–3105

Trojer P and Reinberg D 2006 Histone lysine demethylases and their impact on epigenetics. *Cell* **125** 213–217

Tsuji N, Kobayashi M, Nagashima K, Wakisaka Y and Koizumi K 1976 A new antifungal antibiotic, trichostatin. *J. Antibiot.* **29** 1–6

Ulrich D, Muralitharan R and Gargett CE 2013 Toward the use of endometrial and menstrual blood mesenchymal stem cells for cell-based therapies. *Expert Opin. Biol. Ther.* **13** 1387–1400

van Amerongen R and Nusse R 2009 Towards an integrated view of wnt signaling in development. *Development (Cambridge, England)* **136** 3205–3214

Vasiev B, Balter A, Chaplain M, Glazier JA and Weijer CJ 2010 Modeling gastrulation in the chick embryo: Formation of the primitive streak. *PloS One* **5** e10571

Wang T, Teng S, Zhang Y, Wang F, Ding H and Guo L 2017 Role of mesenchymal stem cells on differentiation in steroid-induced avascular necrosis of the femoral head. *Exp. Ther. Med.* **13** 669–675

Yoshida M, Kijima M, Akita M and Beppu T 1990 Potent and specific inhibition of mammalian histone deacetylase both *in vivo* and *in vitro* by trichostatin A. *J. Biol. Chem.* **265** 17174–17179

Yuan HF, Pan JF, Li S, Guo CA, Liu SH and Yan ZQ 2015 Protective effects of total saponins of panax notoginseng on steroid-induced avascular necrosis of the femoral head *in vivo* and *in vitro. Evidence-based Complement. Altern. Med.: eCAM* **2015** 165679

Zeighami S, Hadjibabaie M, Ashouri A, Sarayani A, Khoee SH, Mousavi S, Radfar M and Ghavamzadeh A 2014 Assessment of cyclosporine serum concentrations on the incidence of acute graft versus host disease post hematopoietic stem cell transplantation. *Iran.J. Pharm. Res.: IJPR* **13** 305–312

Zheng TS, Schlosser SF, Dao T, Hingorani R, Crispe IN, Boyer JL and Flavell RA 1998 Caspase-3 controls both cytoplasmic and nuclear events associated with fas-mediated apoptosis *in vivo. Proc. Natl. Acad. Sci. USA* **95** 13618–13623

Corresponding editor: BJ RAO